Chemical Science

ROYAL SOCIETY OF CHEMISTRY

PERSPECTIVE

View Article Online
View Journal | View Issue

Cite this: *Chem. Sci.*, 2026, **17**, 4846

All publication charges for this article have been paid for by the Royal Society of Chemistry

Innovative chemical design and regulation strategies for overcoming lead toxicity in perovskite-based optoelectronics: a new perspective

Gengling Liu,†[ab] Guo Yang,†[a] Wenhuai Feng†[a] and Wu-Qiang Wu *[a]

The rapid rise of metal halide perovskites has revolutionized optoelectronic technologies, yet the intrinsic lead (Pb) toxicity remains a fundamental challenge threatening environmental safety and sustainable commercialization. This perspective summarizes recent advances over the past two to three years (2023–2025) in innovative chemical design and regulation strategies for Pb sequestration and immobilization within perovskite systems, encompassing both photovoltaic and luminescent devices. Key developments include embedding crosslinked supramolecular networks for Pb capture, constructing supramolecular host–guest inclusion complexes for Pb immobilization, employing chemical synergistic coordination for Pb species stabilization, and achieving lattice-matching anchoring for Pb migration suppression. Dual protection *via* dynamic interfacial confinement and integrated physical–chemical encapsulation further minimizes Pb leakage. In addition, the use of biocompatible supramolecular cyclodextrins for selective Pb ion chelation represents a promising route to reduce Pb toxicity at the material and environmental levels. Despite these achievements, challenges persist in ensuring scalability, long-term stability, and economic feasibility. Looking forward, future efforts should focus on intelligent Pb-sequestrating materials, Pb-free perovskite alternatives, closed-loop recycling systems, and interdisciplinary collaboration. By integrating chemical innovation with sustainability principles, a transformative pathway can be envisioned toward a safe, stable, and environmentally responsible perovskite optoelectronics industry.

Received 19th December 2025
Accepted 2nd February 2026

DOI: 10.1039/d5sc09981a

rsc.li/chemical-science

1 Introduction

Metal halide perovskite-based optoelectronic devices, including solar cells, light-emitting devices, and related technologies, have emerged as leading candidates for next-generation energy conversion and display systems owing to their outstanding

[a]*Key Laboratory of Bioinorganic and Synthetic Chemistry (MoE), Lehn Institute of Functional Materials, School of Chemistry, Sun Yat-sen University, Guangzhou 510006, P. R. China. E-mail: wuwq36@mail.sysu.edu.cn*

[b]*College of Chemistry and Materials Science, Gannan Normal University, Ganzhou, 341000, P. R. China*

† These authors contributed equally to this work.

Gengling Liu

Gengling Liu received his PhD degree from Sun Yat-sen University in 2025. He received his Bachelor's and Master's degrees from Nanchang University in 2018 and 2021, respectively. His recent research interests lie in the design of high-quality perovskite materials and the technical research on the printed fabrication of optoelectronic devices.

Guo Yang

Guo Yang was admitted to the Strengthening Basic Disciplines Plan at Sun Yat-sen University in 2020 and received his bachelor's degree in 2024. He is currently pursuing his PhD at the same institution. His research primarily focuses on the design of high-performance narrow-bandgap perovskite materials and their applications in tandem devices.

device performances, excellent solution processability, and low-cost manufacturing potential.[1–6] However, the most efficient perovskite devices still rely heavily on lead (Pb)-based compositions. The relatively labile Pb–halide coordination bonds in the perovskite lattice can dissociate under environmental stressors such as humidity, thermal cycling, and illumination,[7] resulting in Pb migration and leakage. Such leakage raises serious ecological and toxicological concerns.[8] From an environmental perspective, Pb^{2+} ions exhibit high mobility and bioaccumulation potential. Improper disposal of end-of-life devices may result in Pb^{2+} infiltration into soil *via* rainwater leaching, causing concentrations to exceed regulatory thresholds. Pb contamination not only degrades soil quality but also disrupts water and nutrient uptake in plant roots, ultimately destabilizing agricultural ecosystems.[9] From a health standpoint, Pb is a potent neurotoxin that causes irreversible neurological damage, particularly in children. Bioaccumulation through the food chain or direct exposure poses a severe threat to public health, making Pb contamination a major environmental health issue.[10,11]

To address these risks, multiple research pathways have emerged to mitigate Pb toxicity in perovskite optoelectronics. Most previous studies focused on either physical encapsulation or chemical coordination strategies aimed at suppressing Pb leakage,[12–20] each with inherent limitations. Physical encapsulation approaches, such as the use of ethylene-vinyl acetate (EVA), ionogels, polydimethylsiloxane (PDMS), and UV-curable resins, rely on forming barrier layers over the devices.[21–24] While initially effective in slowing Pb release and protecting perovskite layers from moisture and oxygen, these materials primarily offer mechanical isolation without specific chemical interactions with Pb^{2+} ions. Under prolonged operation, thermal cycling, humidity-induced swelling, or mechanical vibration could induce microcracks and delamination, compromising the encapsulation and increasing the risk of Pb leakage.[25,26] Chemical fixation approaches, on the other hand, rely on specific coordination between Pb^{2+} ions and functional ligands. Small-molecule chelating agents such as ethylenediaminetetraacetic acid (EDTA) could rapidly form stable coordination complexes with Pb^{2+} through multidentate binding, efficiently capturing free ions and reducing their mobility.[27] Other efforts have introduced carboxyl-, amino-, or phosphonic-functionalized molecules capable of forming covalent or coordination bonds with Pb^{2+}. For instance, diphosphatidylglycerol (Di-g) with two phosphonic acid groups has been incorporated at the perovskite/electron transport layer interface, achieving up to 96% suppression of Pb leakage.[28] However, the binding strength and durability of these interactions remain insufficient for long-term operation, as thermal or environmental stress can break coordination bonds or degrade the chelating agents themselves, releasing Pb^{2+} once again. Another direction seeks to eliminate Pb entirely by developing Pb-free perovskite alternatives.[29] Tin-based perovskites, structurally and optoelectronically analogues to their Pb-based counterparts, have attracted extensive interest.[30–33] However, Sn^{2+} is readily oxidized to Sn^{4+}, leading to rapid performance degradation and efficiency loss.[34–36] Similarly, double perovskites and other Pb-free compositions exhibit reduced toxicity but suffer from low carrier mobility (<10 $cm^2\ V^{-1}\ s^{-1}$), which hinders efficient charge transport and limits device performance.[37] Despite significant progress in Pb containment and encapsulation, most approaches remain constrained by their inability to fundamentally alter the chemical state and migration dynamics of Pb within the perovskite lattice. Moreover, Pb leakage suppression is often achieved at the expense of optoelectronic performance. These challenges highlight the urgent need for a paradigm shift from passive Pb capture to active Pb confinement at the source, namely, stabilizing Pb species intrinsically within the perovskite lattice or at key interfaces. This requires innovative chemical and supramolecular design strategies that not only mitigate Pb toxicity but also enhance device performance and stability.

This perspective summarizes recent advances in chemical design and regulation strategies for mitigating Pb toxicity in perovskite-based optoelectronics. It highlights emerging approaches, such as embedding crosslinked supramolecular networks, constructing supramolecular host–guest inclusion complexes, employing chemical synergistic stabilization, defect trapping and self-healing, lattice-matching anchoring, dynamic interfacial confinement, and integrated physical–chemical dual

Wenhuai Feng

Wenhuai Feng received his PhD degree from Sun Yat-sen University in 2024. He received his Master's degree from Fujian Normal University in 2019 and Bachelor's degree from Gannan Normal University in 2016. His recent research interests lie in the design of device configurations and high quality perovskite crystal materials and their applications in scalable fabrication of optoelectronic devices.

Wu-Qiang Wu

Wu-Qiang Wu received his PhD degree from the University of Melbourne in 2017. He received his Bachelor's and Master's degrees from Sun Yat-sen University in 2011 and 2013, respectively. His current research interests lie in the fabrication of functional optoelectronic materials and their applications in perovskite solar cells, light-emitting devices and wearable optoelectronics.

protection. Together, these strategies illustrate a new materials design philosophy that combines supramolecular chemistry with sustainability principles to balance toxicity control and device optimization. Finally, this perspective discusses the remaining challenges in scalability, stability, and cost-effectiveness, and outlines future research directions toward intelligent Pb-sequestrating materials, environmentally benign alternatives, and closed-loop recycling, ultimately aiming to achieve safe, sustainable, and high-performance perovskite optoelectronics.

2 State-of-the-art strategies for lead sequestration and immobilization

Supramolecular engineering offers unique advantages for environmentally safe perovskite optoelectronics, including precise molecular recognition, the ability to form stable host–guest complexes, and the potential for multi-point interactions tailored to specific targets such as Pb^{2+} ions.[38] These features not only enable multi-defect passivation but also enhance material stability and facilitate efficient Pb sequestration and immobilization, often throughout the entire process from perovskite precursor solutions to thin films and final devices.[39,40] Among the diverse candidates of macrocyclic supramolecular hosts, cyclodextrins (CDs) stand out due to their unique molecular architecture and significant potential as functional materials.[41] CDs are biocompatible macrocyclic oligosaccharides composed of α-1,4-linked glucopyranose units, forming a truncated cone with a hydrophobic cavity and a hydrophilic hydroxyl-rich exterior.[42] This structural motif directly imparts three key functionalities for Pb^{2+} management in perovskite optoelectronics: (1) molecular encapsulation or host–guest interactions with Pb^{2+} or Pb-containing species *via* cluster or cross-linked networks; (2) multidentate chelation of Pb^{2+} through abundant surface hydroxyl groups; and (3) inherent biocompatibility with minimal environmental impact. Leveraging the tunable nature of supramolecular chemistry and the intrinsic advantages of CDs, our team and others have developed a series of innovative design strategies.

2.1 Cross-linked cyclodextrin supramolecular networks

First, a robust cross-linked supramolecular network was constructed *via* a dehydration esterification reaction between 2-hydroxypropyl-β-cyclodextrin (HPβCD) and 1,2,3,4-butanetetracarboxylic acid (BTCA).[43] This network forms multi-dimensional Pb^{2+} capture sites *via* abundant chemical interactions, thereby enabling efficient anchoring of free Pb^{2+} within the perovskite lattice (Fig. 1a). To evaluate the Pb leakage suppression capability of HPβCD-BTCA, its Pb chelating capacity was first tested in solution. When 0.4 mol% HPβCD-BTCA was added to 10 mL of deionized water containing 1.93×10^{-2} mM PbI_2 (~4000 ppb Pb), the Pb^{2+} concentration decreased sharply. After 90 minutes, the Pb^{2+} level dropped to 67 ppb (Fig. 1b), well below China's wastewater total Pb standard (≤1000 ppb).[44] Subsequently, the Pb leakage from damaged perovskite solar cells (PSCs) with or without a built-in crosslinked HPβCD-BTCA network was compared (Fig. 1c). Using inductively coupled plasma mass spectrometry (ICP-MS), devices with only epoxy-sealed glass exhibited a continuous increase in Pb^{2+} concentration during water rinsing, whereas HPβCD-BTCA-modified devices reached near-saturation within 10 minutes and showed negligible further increase even after 1 hour. This indicates that early-released soluble Pb^{2+} ions were effectively captured by the cross-linked network, preventing environmental release. After 60-minute water rinsing, the Pb^{2+} leakage rate decreased from 973 mg m^{-2} h^{-1} for the control to 54 mg m^{-2} h^{-1} for the modified device, corresponding to a Pb sequestration efficiency of 94.5% (Fig. 1d). Recognizing that device failure often results from water-induced perovskite decomposition or glass fragments puncturing functional layers under extreme conditions, we further optimized the encapsulation by replacing the cover glass with a flexible polymer sheet incorporating HPβCD-BTCA electrospun onto a polystyrene scaffold (device III in Fig. 1c). This flexible sheet further reduced Pb leakage during water exposure while simultaneously enhancing mechanical impact resistance. The optimized device achieved a Pb leakage rate of 14 mg m^{-2} h^{-1} (98.6% sequestration efficiency), with only 14 ppb Pb^{2+} detected after 60 minutes of water rinsing, below the US EPA action level for drinking water (15 ppb).[45] Compared with reported Pb adsorbents, the key advantage of this cross-linked HPβCD-BTCA supramolecular network lies in its dual-capture mechanism: strong chemical adsorption through multiple chemical interactions and physical confinement *via* HPβCD cavities and/or interconnected nano-/mesopores of the network (Fig. 1e). This synergistic chemical–physical mechanism offers a promising solution for highly efficient Pb leakage suppression. Besides, devices with integrated HPβCD-BTCA networks and flexible sheets (device III) retained 97% of their initial efficiency after continuous water rinsing for 522 hours (Fig. 1f). Notably, HPβCD-BTCA also stabilized perovskites at the precursor stage by forming hydrogen bonding interactions with I^- in formamidinium iodide (FAI), inhibiting FAI deprotonation and suppressing the formation of *s*-triazine impurities, thereby enhancing the photo-, thermal-, and humidity stability of perovskite films and devices (Fig. 1g). The champion PSC efficiency improved from 20.52% (control) to 22.14%. Overall, this cross-linked supramolecular strategy enables multidimensional control from precursor stabilization to device performance enhancement and Pb^{2+} capture, offering a practical and innovative solution to perovskite Pb^{2+} leakage. Its core value lies in overcoming the traditional trade-off between toxicity suppression and performance optimization, paving the way for sustainable commercialization of perovskite photovoltaics.

2.2 Cyclodextrin supramolecular host–guest complexes

For flexible, Pb-based perovskite wearable optoelectronics, Pb^{2+} leakage remains a critical environmental bottleneck. It is worth mentioning that Pb-release risks and dominant stressors are application-dependent. For instance, photovoltaic modules are often governed by rainwater leaching after encapsulation damage, whereas light-emitting and wearable devices may face repeated mechanical abrasion and dynamic water/seawater

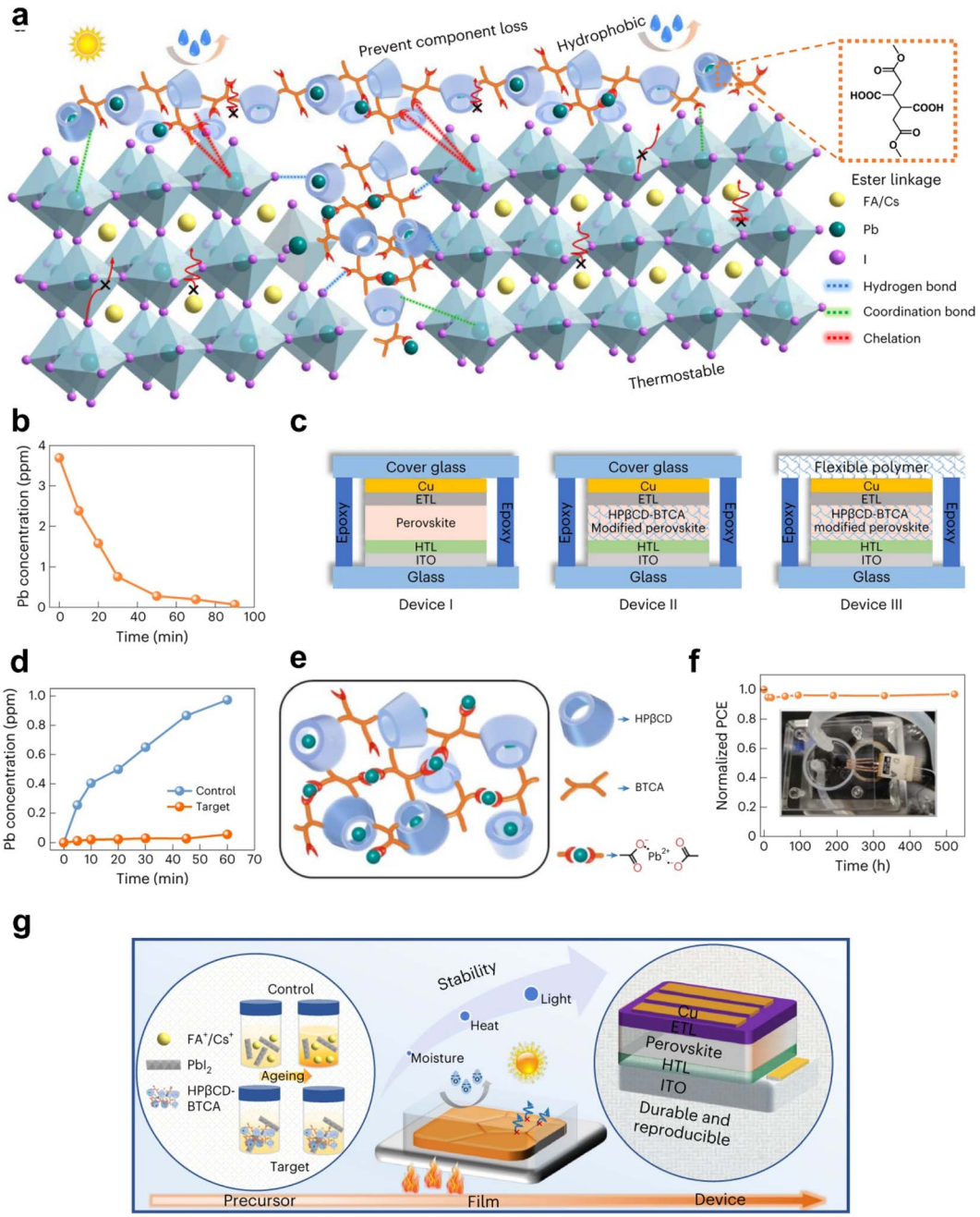

Fig. 1 (a) Schematic illustration of chemical interactions between the cross-linking HPβCD-BTCA supramolecular complex and perovskite and the advantages in terms of improving water resistance and thermal stability, preventing component loss and mitigating ion migration. (b) Demonstration of the Pb-adsorbing capabilities of the HPβCD-BTCA complex. (c) Schematic illustration of device configurations (devices I, II and III) with different perovskite films and encapsulation modes. (d) Comparison of Pb^{2+} sequestration in damaged PSCs with or without HPβCD-BTCA. (e) Schematic illustration of Pb^{2+} capture by the cross-linked HPβCD-BTCA supramolecular network. (f) PCE evolution of broken PSCs under dynamic water scouring for 522 h. (g) Schematic illustration of the HPβCD-BTCA-assisted stabilization throughout the entire fabrication process from the perovskite precursor to the intermediate film and to the final device. ITO: indium-doped tin oxide; ETL: electron transport layer; HTL: hole transport layer. Reprinted with permission.[43] Copyright © 2023 Springer Nature Limited.

scouring. Accordingly, Pb-leakage mitigation strategies should be benchmarked under different stress conditions that match the intended deployment scenario. We designed a composite fiber structure comprising a polymer matrix, HPβCD, and a fluorinated hydrophobic agent (perfluorooctyltriethoxysilane, PFOS), employing host–guest interactions and multi-layer protection for efficient Pb^{2+} immobilization.[46] The multidentate hydroxyl groups of CDs form stable host–guest complexes with Pb^{2+} in perovskites, simultaneously passivating crystallographic defects and anchoring Pb^{2+} within the cavity of CD clusters, thereby reducing the release of free Pb^{2+} (Fig. 2a). Superhydrophobic fluorinated silane on the fiber exterior forms

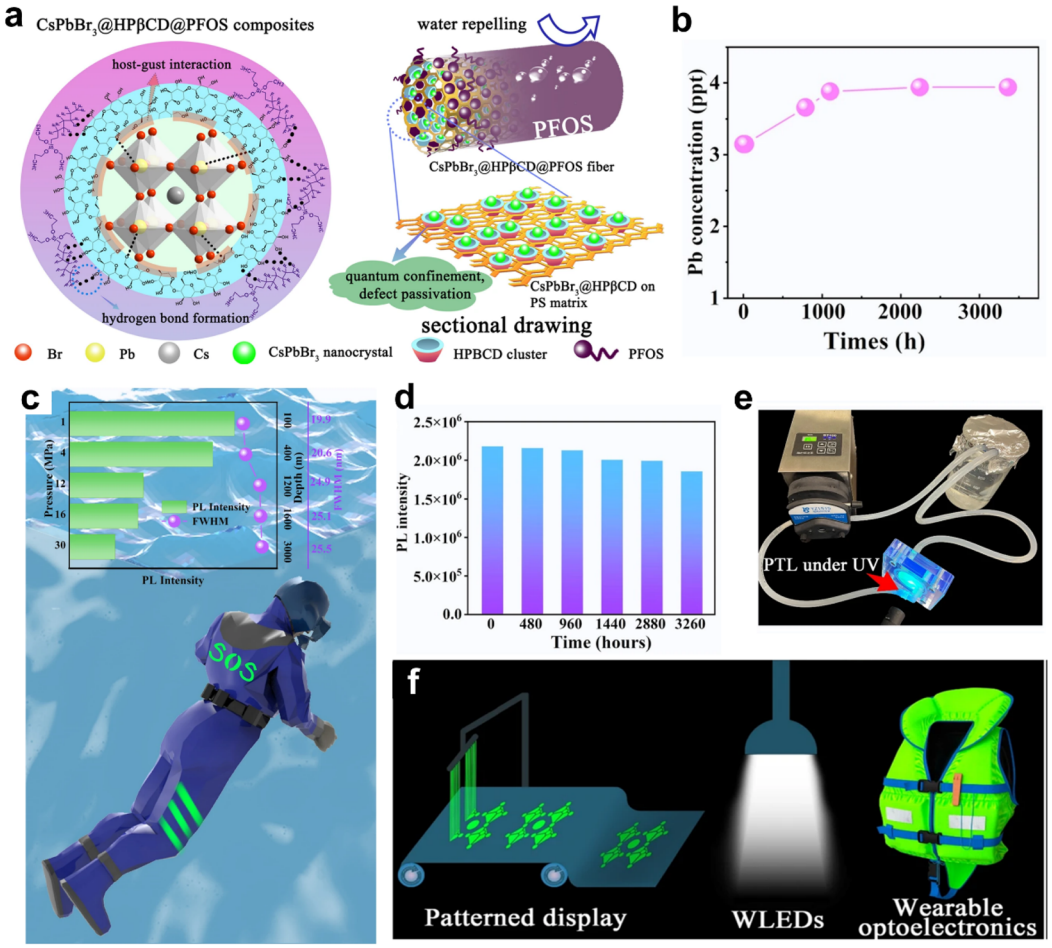

Fig. 2 (a) Schematic illustration of the chemical interactions in $CsPbBr_3$@HPβCD@PFOS composites and their multifaceted functions. (b) Trace of leaked Pb ion concentrations over extended water scouring time. (c) Evolution of PL intensity and FWHM of $CsPbBr_3$@HPβCD@PFOS-based PLTs as a function of pressure and depth, alongside a schematic of an "SOS" signal patterned on a life jacket fabricated with $CsPbBr_3$@HPβCD@PFOS fibers. (d) Evolution of PL intensity of $CsPbBr_3$@HPβCD@PFOS-based PLTs during 3260 h of water immersion. (e) The setup to simulate the real conditions of PLTs under dynamic seawater scouring. (f) Applications of $CsPbBr_3$@HPβCD@PFOS composites in patterned displays, white light-emitting diodes (WLEDs) and wearable optoelectronics. Reprinted with permission.[46] Copyright © 2023 Springer Nature Limited.

strong hydrogen bonds with CDs, constructing a physical barrier that prevents moisture intrusion-induced perovskite decomposition and blocks the migration path of Pb^{2+}. This synergistic design affords excellent Pb leakage suppression. After dynamic water scouring for more than 3300 hours, only 3.94 ppt of Pb^{2+} leaching was detected (Fig. 2b), far below the World Health Organization's standard for Pb content in drinking water (<10 ppb), solving the limitations of conventional polymer-encapsulated perovskites. The multi-layer structure of the composite fibers also imparts remarkable environmental stability, withstanding prolonged water immersion (>3300 h) and pressures up to 30 MPa (Fig. 2c and d). The extrapolated photoluminescence half-life (T_{PL50}) under ambient conditions reached 14 193 h. A home-made apparatus was used to simulate the real conditions of PLTs under dynamic seawater scouring at a fast flow rate of 570 mL min^{-1}, during which the PLTs could continuously emit green light upon excitation (Fig. 2e). The composite fiber exhibited excellent luminescent properties with a photoluminescence quantum yield (PLQY) of 49.7% and a full-width at half-maximum (FWHM) <17 nm, suitable for patterned displays, white LEDs, and wearable marine rescue devices (Fig. 2f). The core value of this strategy lies in realizing extreme suppression of Pb leakage in flexible perovskite luminescent textiles through the combination of host–guest chemistry and physical encapsulation, while simultaneously achieving efficient photoluminescence, as well as remarkable environmental stability and safety. It opens up a new path for the environmentally friendly application of Pb-based perovskite materials. Similarly, Chen *et al.* demonstrated that β-CD could serve as an effective Pb^{2+} leakage suppressor in 2D perovskite films and devices.[47] In water immersion tests, control films released ~40 000 ppb (40 ppm) Pb^{2+} in 70 min, whereas β-CD-modified films released only 8300 ppb (8.3 ppm), reducing leakage rates significantly. Addition of 5% β-CD decreased dissolved Pb^{2+} from 7600 ppb (7.6 ppm) to 1600 ppb (1.6 ppm) in 90 min. Structurally, the β-CD-modified films maintained integrity in water for over 30 s, far exceeding the control films' 3 s, confirming the formation of

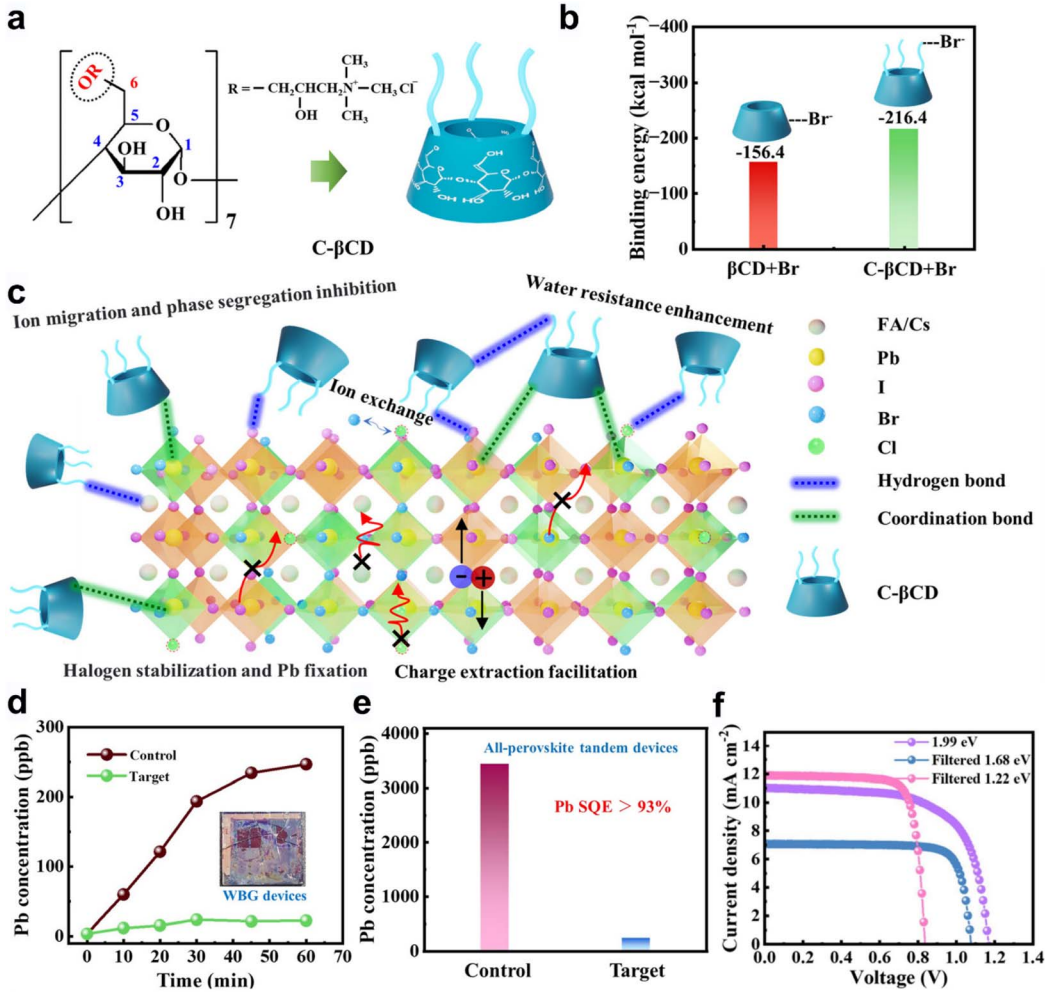

Fig. 3 (a) Molecular structure of C-βCD. (b) Calculated binding energies between βCD and Br^- and between C-βCD and Br^-. (c) Schematic illustration of chemical interactions (*i.e.* hydrogen bonding, coordination bonding and/or ion exchange) between C-βCD and I/Br-based WBG perovskites and the advantages in terms of water resistance enhancement, ion migration and phase segregation inhibition, halide stabilization and Pb fixation, as well as charge extraction facilitation. (d) Comparison of Pb leakage content for the damaged control and target WBG PSCs. (e) Comparison of Pb leakage content for the control and target 4T all-perovskite TSCs (with both sides severely broken). (f) *J*–*V* curves of 1.99 eV WBG PSC, filtered 1.68 eV WBG PSC, and filtered 1.22 eV NBG PSC. Reprinted with permission.[48] Copyright © 2025 Wiley-VCH GmbH.

a chemical–physical dual barrier enhancing environmental safety.

2.3 Functionalized cyclodextrin derivatives for chemical synergistic coordination

Rational molecular design of functionalized cyclodextrin derivatives offers opportunities to extend Pb^{2+} leakage suppression across diverse perovskite compositions. In tandem solar cells (TSCs) using wide-bandgap (WBG, 1.6–2.0 eV) mixed-halide perovskites with high Br contents, which are more prone to Pb leakage due to exacerbated halide segregation, phase separation, and ion migration, we developed a chemical synergistic stabilization strategy using cationic β-cyclodextrin (C-βCD), further expanding the application scenarios of CDs in Pb leakage suppression.[48] C-βCD also relies on the cavity structure to achieve host–guest interactions (Fig. 3a). Interestingly, the cationic functionalization could strengthen affinity toward halide ions in high-Br-content WBG perovskites (Fig. 3b). C-βCD exerted a chemical synergistic effect as follows: the hydroxyl groups coordinated Pb^{2+}, while quaternary ammonium cations interacted electrostatically with Br^-/I^- and Cl^-, inducing favorable halide ion exchange with perovskites, thereby stabilizing both halides and Pb^{2+} and mitigating lattice degradation-induced Pb^{2+} leakage (Fig. 3c). Pb leakage tests revealed that severely damaged single-junction WBG PSCs released only 5.63 ppb (Fig. 3d), which is far below the U.S. safe drinking water standard (<15 ppb). Even under extreme conditions (double-sided damage in four-terminal tandem solar cells), the Pb sequestration efficiency remained as high as 93.4% (Fig. 3e). Notably, the C-βCD strategy also inhibited light-induced halide segregation and phase separation, boosting the efficiency of WBG PSCs by 10–36%. And the all-perovskite TSCs achieved efficiencies of 24.39% (4T) and 22.42% (6T) (Fig. 3f), respectively.

Similarly, under the design principle of a "CD" scaffold with tunable functional groups, Wang *et al.* grafted seven thiol (–SH)

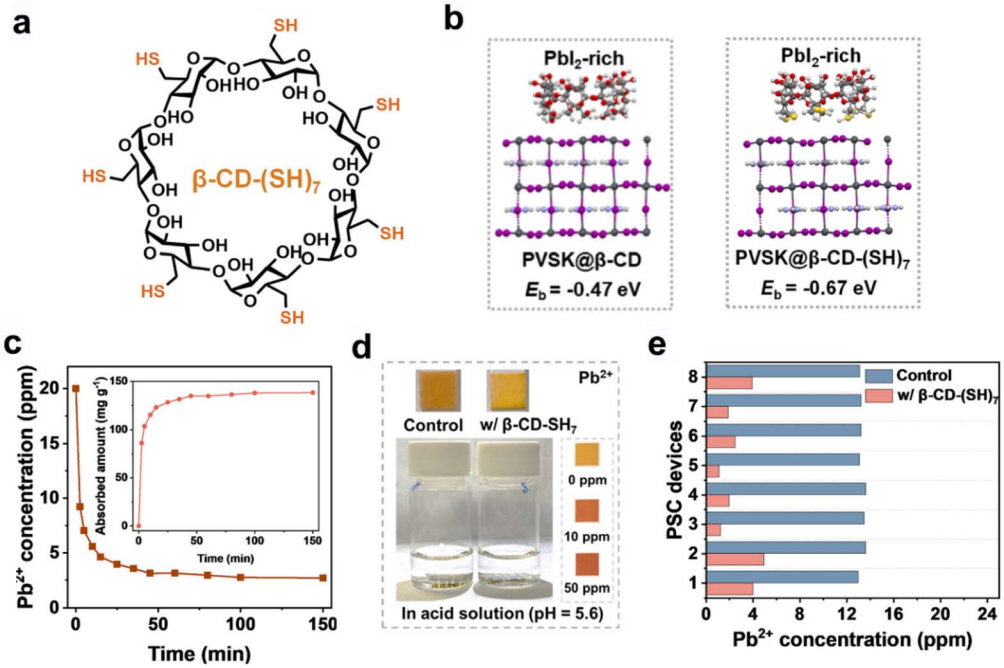

Fig. 4 (a) Molecular structure of thiol-functionalized β-CD-$(SH)_7$. (b) Optimized slab structures and calculated binding energy (E_b) of β-CD (left) and β-CD-$(SH)_7$ (right) on a PbI_2-rich perovskite surface. (c) Pb^{2+} sorption kinetics of β-CD-$(SH)_7$ (2.5 mg) at an initial Pb^{2+} concentration of 20 000 ppb (20.0 ppm). The inset shows the corresponding absorbed Pb^{2+} amount. (d) The Pb concentration in the deionized water, which is quickly detected by Pb ion testing paper. The degraded devices are immersed for 15 min. (e) Pb^{2+} concentration in contaminated water measured by ICP-OES. Reprinted with permission.[49] Copyright © 2025 Elsevier.

groups onto β-CD to synthesize β-CD-$(SH)_7$ (Fig. 4a). The high-density thiols provide additional Pb^{2+} binding sites,[49] as confirmed by theoretical calculations showing a substantially enhanced binding energy of β-CD-$(SH)_7$ with Pb^{2+} compared to unmodified β-CD (Fig. 4b), enabling *in situ* adsorption of Pb^{2+} released during perovskite degradation. Quantitative analysis demonstrated that β-CD-$(SH)_7$ possessed outstanding Pb adsorption performance, characterized by an adsorption capacity (q_e) of 139.66 mg g^{-1} and a first-order adsorption rate constant of 0.047 min^{-1} (Fig. 4c). To simulate the degradation behavior of PSCs under acid rain conditions, the devices were immersed in acid water with a pH of 5.6 (Fig. 4d). The results confirmed effective Pb^{2+} leakage suppression, with average Pb^{2+} concentration <5000 ppb (5 ppm) in β-CD-$(SH)_7$-modified devices *versus* 13 000 ppb (13 ppm) in controls (Fig. 4e). In fact, beyond reducing the released Pb concentration, future "detoxification" designs should explicitly report Pb speciation and ecotoxicity endpoints (*e.g.*, algae/soil microorganism assays), because chelation-driven immobilization does not automatically guarantee biological benignity under diverse environmental conditions.

2.4 Macrocyclic metalloporphyrins for lattice-matched coordination

The series of cyclodextrin-based strategies described above work effectively across pure Pb-based perovskites with different bandgaps, showing excellent suppression of Pb leakage. Beyond cyclodextrins (CDs), other cyclic molecules such as macrocyclic metalloporphyrins, have also been innovatively applied to mitigate Pb leakage, particularly in narrow-bandgap Sn–Pb alloyed perovskites. In these compositions, differences in the crystallization kinetics of Sn^{2+} and Pb^{2+} lead to enrichment of Pb^{2+} at the buried interface, raising the risk of Pb release when devices are damaged.[16] We proposed a lattice-matched coordination strategy using a spider-web-like quadrilateral macrocyclic metalloporphyrin (TAPP-Zn) (Fig. 5a). The key mechanism operates through two features: (i) the molecular dimensions of TAPP-Zn closely matched the lattice of Sn–Pb perovskites (the spacing between the amino groups is twice the size of the perovskite unit cell, Fig. 4b); (ii) TAPP-Zn exhibited preferential coordination toward Pb^{2+} (Fig. 5c). Through its four amino groups, TAPP-Zn formed strong coordination bonds with Pb^{2+} and simultaneously modulated crystallization kinetics, increasing the surface Pb abundance by 61%, altering the spatial distribution of Pb^{2+} in the film, and reducing Pb accumulation at the buried interface (Fig. 5d). This lattice-matched, targeted coordination enabled effective Pb immobilization and inhibited Pb leakage (Fig. 5e). After being severely damaged and immersed in water for 150 hours, the TAPP-Zn-modified Sn–Pb PSCs exhibited only 1.23 ppb of Pb leakage, representing a 24-fold reduction in the leakage rate (Fig. 5f), significantly improving the environmental safety. In addition to efficiently suppressing Pb leakage, this strategy also offers multiple additional values. Firstly, the coordination interaction of TAPP-Zn enhanced the chemical homogeneity of Sn–Pb perovskites, reduced defect-state density, relieved tensile strain, and optimized carrier dynamics, enabling a single-junction PSC efficiency of 23.28% (Fig. 5g). Secondly, for tandem applications,

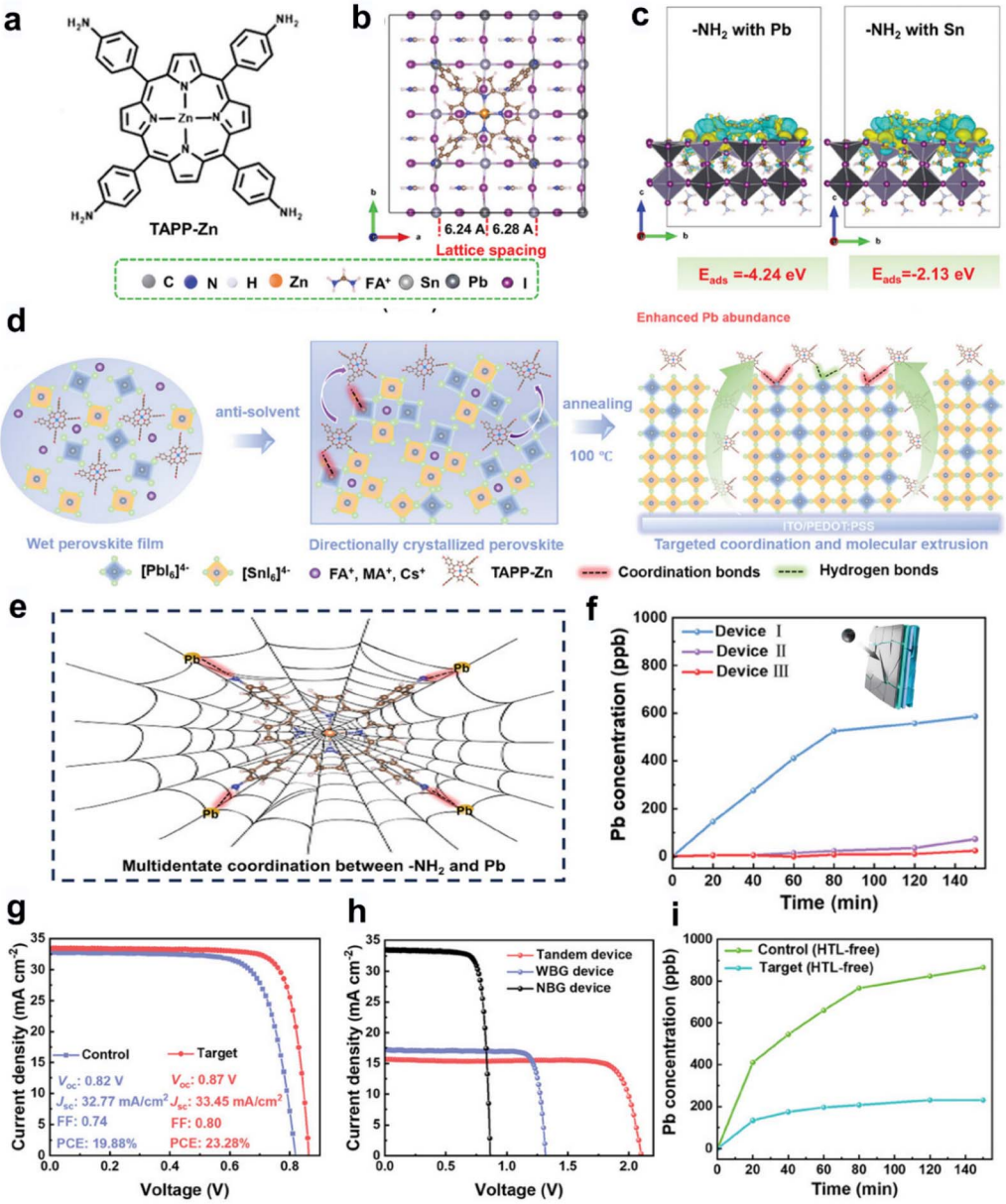

Fig. 5 (a) Molecular structure of the TAPP-Zn macrocyclic molecule. (b) Lattice structure of Sn–Pb alloyed perovskite showing TAPP-Zn binding with four Pb atoms. (c) Calculated adsorption energies of $-NH_2$ groups in TAPP-Zn to the $[PbI_6]^{4-}$ and $[SnI_6]^{4-}$ octahedra of the perovskite. (d) Schematic diagram of TAPP-Zn-assisted crystallization and metal ion distribution during the formation of Sn–Pb alloyed perovskite films. (e) Schematic of the coordination-driven immobilization of leaked Pb^{2+} ions by TAPP-Zn. (f) Time-dependent Pb concentration evolution in contaminated water derived from three types of severely damaged devices (inset illustrates the damage incurred from the back-electrode side). (g) *J*–*V* curves of the control and target TAPP-Zn-modified PSCs. (h) *J*–*V* curves of single-junction WBG and NBG PSCs and integrated all-perovskite TSCs. (i) Time-dependent Pb concentration evolution in contaminated water derived from damaged HTL-free PSCs with or without TAPP-Zn modification. Reprinted with permission.[16] Copyright © 2024 Wiley-VCH GmbH.

monolithic all-perovskite TSCs prepared using this strategy achieved a PCE of 27.03% with excellent photostability (Fig. 5h). Thirdly, the strategy demonstrated high generality by remaining effective even in HTL-free Sn–Pb PSCs. The modified HTL-free device achieved a PCE of 21.34%, representing an approximately 30% improvement over the unmodified control (16.56%). The Pb concentration in contaminated water from the unmodified HTL-free control PSCs was determined to be 866.3 ppb, whereas that from the target HTL-free PSCs was significantly reduced to 230.6 ppb (Fig. 5i). This result further verifies the strategy's potential for simplifying device structures, reducing production costs and enhancing the environmental viability. Overall, the TAPP-Zn strategy used lattice-matched coordination and preferential binding with Pb^{2+} to specifically address the Pb leakage challenge in Sn–Pb alloyed perovskites. It not only validates the core concept of "chemically immobilizing Pb^{2+} ions through coordination", but also expands its applicability to multi-metal-cation perovskites through

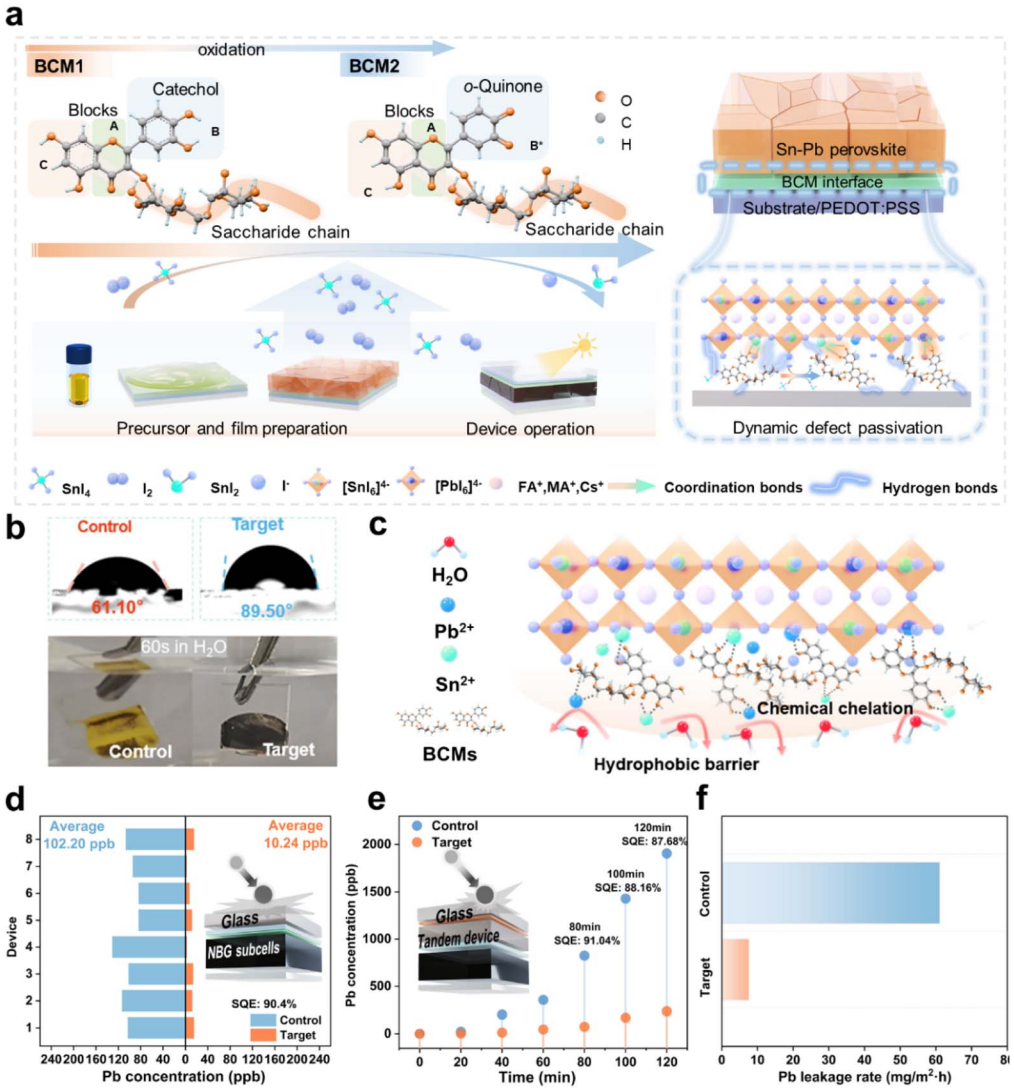

Fig. 6 (a) Schematic illustration of the oxidation-triggered transformation from BCM1 to BCM2 and its role as a buried interface modifier for Sn–Pb perovskites. (b) Contact angles of water droplets on the control and target perovskite buried interfaces, and photographs of the corresponding films upon immersion in water for 60 s. (c) Schematic illustration of BCM-assisted water resistance enhancement and chemical chelation-assisted Pb leakage suppression at the perovskite buried interface. (d) Pb leakage concentrations from the damaged control and target NBG subcells after 2 h of simulated rainwater washout. (e) Time-dependent Pb leakage profiles of damaged control and target BCM-modified tandem PSMs during 2 h of simulated rainwater washout. (f) Comparison of Pb leakage rates from damaged control and target BCM-modified tandem PSMs after 2 h of simulated rainwater scouring. Reprinted with permission.[6] Copyright © 2025 Wiley-VCH.

molecular structure innovation, providing a new pathway toward environmentally safe deployment of Pb-based perovskites in all scenarios. Although TAPP-Zn effectively modulates Pb^{2+} spatial distribution and inhibits leakage, its coordination-driven approach still faces scale-up and durability challenges. The uniform dispersion of TAPP-Zn and its interaction stability within hybrid perovskite matrices under prolonged light and thermal stress require further investigation. Additionally, possible impacts on charge transport and interfacial energy alignment should be carefully evaluated before integration into large-size modules.

Hole-transport-layer-free carbon-based perovskite solar cells (HTL-free C-PSCs) also face unresolved environmental risks. To address this, Zhong *et al.* introduced a fluorinated lead-chelating (FLC) molecule (potassium trifluoromethanesulfonate) at the perovskite/carbon interface.[50] The exceptional Pb^{2+} retention capability originated from the strong chelation interaction between trifluoromethanesulfonate anions and undercoordinated Pb^{2+} species, which stabilized the perovskite lattice structure. Furthermore, the hydrophobic $-CF_3$ functional groups synergized with the intrinsic hydrophobicity of the carbon electrode to effectively block water ingress. Collectively, these effects significantly suppressed moisture-triggered perovskite degradation and Pb^{2+} migration, thereby providing robust environmental stability. This strategy effectively reduced Pb leakage in acidic aqueous environments, lowering the Pb leakage rate from 334.7 mg m^{-2} h^{-1} to 53.7 mg m^{-2} h^{-1} and achieving a Pb

sequestration efficiency of approximately 84%. These findings highlighted the potential of FLC molecules interfacial modification in enabling environmentally safer HTL-free C-PSCs, even under extreme operational scenarios, thereby advancing their viability for real-world deployment.

2.5 Oxidation-triggered enhanced Pb immobilization using multifunctional rutin-based blockchain molecules

Building on the successful mitigation of Pb leakage in pure-Pb, Sn–Pb mixed-perovskites, and various single-junction device architectures, increasing attention has turned to Pb containment in tandem devices. Recently, we developed an innovative dynamic buried interface engineering strategy utilizing biocompatible, multifunctional rutin-based blockchain molecules (BCM1) for achieving full-lifecycle management of NBG subcells and their corresponding tandem solar modules (TSMs).[6] This approach covered fabrication, operation, and post-damage stages, aiming to resolve the intertwined challenges of efficiency, stability, and sustainability in all-perovskite tandem photovoltaics. During device fabrication or processing, the catechol groups in BCM1 can be oxidized by Sn^{4+} and I_2 into o-quinone-containing oxidized rutin (BCM2), which exhibited significantly enhanced chelating ability. This oxidation established a sustained dynamic passivation and protection mechanism at the buried interface (Fig. 6a). Hydroxyl and carbonyl groups, as well as the saccharide chains on BCM1/MCM2 formed synergistic interactions with undercoordinated Sn^{2+}/Pb^{2+} ions at the perovskite buried interface, while also creating hydrogen-bond networks that anchored iodide ions, enabling both crystallization regulation and persistent defect passivation. More importantly, this molecular transformation increased the proportion of non-polar aromatic domains and the surface area of the hydrophobic carbon framework. When Sn–Pb perovskite buried-interface films were immersed in water, control films rapidly turn from black to yellow (indicative of accelerated decomposition), whereas BCM2-protected films remained black even after 60 seconds (Fig. 6b). Binding-energy calculations showed that the interaction energies between Pb^{2+} and water were −0.598 eV for the control and −0.082 eV for the treated film, while Pb^{2+}–BCM2 interaction energy was −0.996 eV, demonstrating that BCM2 binded Pb^{2+} far more strongly than water does, effectively blocking Pb^{2+}–water interactions. This dual mechanism, namely, hydrophobic protection and chemical coordination, greatly enhanced Pb-leakage suppression under simulated heavy-rain conditions (Fig. 6c). In damaged NBG sub-cells, the average Pb^{2+} concentration from BCM-modified devices was only 10.24 ppb, far below the control group (102.21 ppb) and compliant with the U.S. EPA standard (<15 ppb), corresponding to a sequestration efficiency (SQE) of 90.4% (Fig. 6d). After 80 minutes of testing, BCM-modified TSMs still achieved a sequestration efficiency of 91.04% (73.90 ppb *vs.* 824.97 ppb in controls), and retained ∼87.68% even after 120 minutes (Fig. 6e). Moreover, the Pb-leakage rate drops dramatically from 61.06 mg m^{-2} h^{-1} (control) to 7.58 mg m^{-2} h^{-1} with BCM protection (Fig. 6f), extending the recovery window for damaged devices and reducing environmental impact. Encouragingly, after optimization, small-area (0.045 cm^2) and large-area (10.4 cm^2) NBG single-junction devices achieved efficiencies of 23.50% and 17.10%, respectively. All-perovskite TSMs (10.4 cm^2) attained a 23.00% aperture efficiency (an active-area efficiency of 24.30%), retaining ∼90% of their initial efficiency after 640 h of continuous operation under one-sun illumination (extrapolated T_{PCE80} lifetime of 3900 h) and demonstrating 90% efficiency retention after 15 cycles of day–night fatigue tests, placing these devices among the top-performing tandem photovoltaic modules reported to date.

3 Chelation of lead ions for reduced lead toxicity

Conventional Pb-leakage mitigation methods mainly rely on physical barriers or single-mode chemical adsorption, which could not fundamentally address the intrinsic biological toxicity of Pb^{2+}. Although Pb-adsorbing materials could significantly reduce the amount of Pb released from PSCs, the adsorption products themselves still contain Pb and thus pose risks of secondary contamination. The key issue is that the chemically immobilized Pb^{2+} ions on these adsorbents may re-dissolve or diffuse back into the environment, especially once adsorption sites become saturated or chemically deactivated. At the same time, toxic Pb species can enter water systems or accumulate through food-chain transfer, creating severe biological-magnification hazards to human health. Therefore, reducing Pb toxicity is as essential as minimizing Pb leakage when developing environmentally friendly perovskite photovoltaics.

Notably, we achieved an important breakthrough by using biocompatible supramolecular cyclodextrins (CDs) to mitigate Pb toxicity. Leveraging the high Pb-chelation capability of CDs, we significantly enhanced the biocompatibility of Pb-based perovskites.[43] Specifically, HPβCD-BTCA provided densely distributed hydroxyl and carboxyl coordination sites that form multidentate chelation with Pb^{2+} (Fig. 1e), making it extremely difficult for Pb^{2+} to re-dissociate and be released. This process simultaneously achieves "chemical detoxification" of Pb^{2+}. The chelation not only immobilizes Pb^{2+} but also alters its chemical speciation. The water solubility of the HPβCD-BTCA@Pb^{2+} complex is greatly reduced (Fig. 7a), effectively blocking the pathways through which Pb^{2+} ions would otherwise enter biological systems *via* water or food chains. In addition, introducing biocompatible CDs provided unique advantages for managing Pb toxicity in perovskite optoelectronic devices. We systematically verified, for the first time, the biocompatibility of HPβCD-BTCA-modified perovskite films. Using *Escherichia coli* (*E. coli*) as a model microorganism, we assessed the influence of Pb-containing perovskites on bacterial growth and proliferation. Previous studies show that heavy metals such as Pb significantly inhibited *E. coli* growth. Thus, we immersed perovskite films into bacterial culture media and monitored the optical density at 600 nm (OD_{600}, the characteristic absorption peak of *E. coli*) throughout the incubation period to quantify bacterial growth kinetics (Fig. 7b). The results showed that unmodified perovskites strongly inhibited bacterial growth,

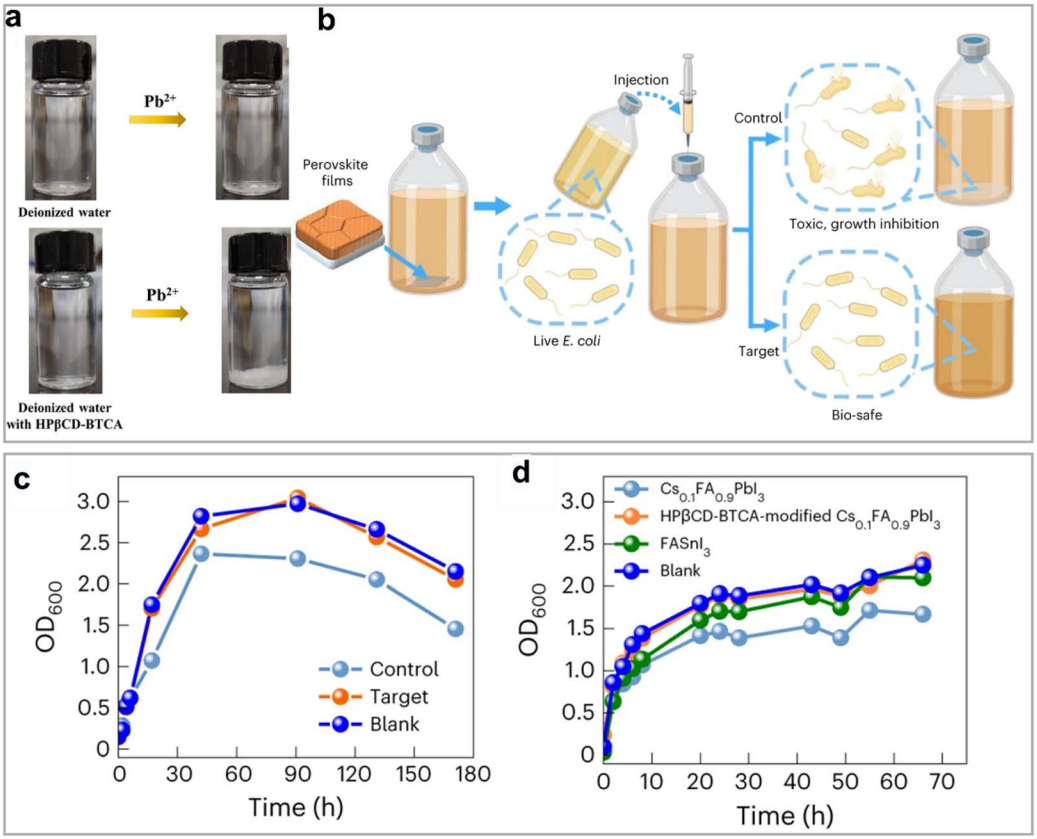

Fig. 7 (a) Photographs of deionized water (DI water) and HPβCD-BTCA aqueous solutions (0.4 mol% HPβCD-BTCA in DI) before (left) and after (right) adding Pb^{2+} ions (PbI_2 was used as the Pb source). (b) Schematic illustration of preparing *E. coli* culture solution with perovskite incorporation and the impact of different perovskites on the growth performance of *E. coli* over time. (c) The impact of control or target perovskites on the growth performance of *E. coli* (BNCC133264, BeNa Culture Collection), monitored by the change of optical density at 600 nm (OD_{600}) over time. (d) Effects of different perovskite compositions and components on growth performance of *E. coli*. Reprinted with permission.[43] Copyright © 2023 Springer Nature Limited.

while the HPβCD-BTCA-modified perovskites produced growth curves nearly identical to the blank control, demonstrating that Pb^{2+} chelated by HPβCD-BTCA exhibited excellent biocompatibility, comparable to lead-free Sn-based perovskites (Fig. 7c and d). These results confirmed that employing low-cost, biocompatible CDs supramolecules for managing Pb toxicity in high-performance PSCs provides substantial ecological benefit. While HPβCD-BTCA demonstrates remarkable Pb^{2+} immobilization and biocompatibility, its practical translation may face certain challenges. The performance strongly depends on the uniform distribution and stable crosslinking of HPβCD-BTCA within bulk perovskite films and multilayer device architectures, which could be more difficult to maintain under large-area coating or long-term thermal cycling. Moreover, the long-term chemical integrity (*i.e.* ionic strength) of the CD-Pb complexes under realistic environmental fluctuations (*e.g.*, pH variation and multiple wet–dry cycles) remains to be systematically validated.

Inspired by toxicity studies using *E. coli* as an investigation subject, other researchers have also developed a more multi-dimensional evaluation system for assessing the ecological impact of Pb leakage from perovskite optoelectronic devices. Very recently, Hu and colleagues introduced environmentally friendly hydroxypropyl methylcellulose phthalate (HPMCP) into the perovskite layer, leveraging its multiple adsorption modes and sites (forming coordination bonds and hydrogen bonds with perovskites through functional groups such as C=O, C–O, and –OH) to suppress Pb leakage.[51] They systematically compared the effects of HPMCP-modified, polydimethylsiloxane (PDMS)-modified, and unmodified lead-based perovskite films on the survival of adipose-derived stem cells, soil ecosystems, and plant growth and germination (Fig. 8a). Through the synergistic effect of its multifunctional groups, HPMCP demonstrated excellent performance in inhibiting lead leakage and toxicity. In cell experiments, the unmodified film group showed severe lead leakage, with only 2.89% cell survival after 7 days. In contrast, the HPMCP and PDMS groups maintained high cell survival rates of 95.29% and 93.45%, respectively, comparable to the lead-free counterpart group (Fig. 8b). Soil burial experiments revealed that unmodified perovskite rapidly and continuously released lead ions. The PDMS-modified group exhibited slower but gradually increasing release, while the HPMCP-modified group stabilized after an initial slow release (Fig. 8c). In plant experiments using radish, the germination rate was 0% for the unmodified group, 50% for the HPMCP group (close to 55% in the control group), and 45%

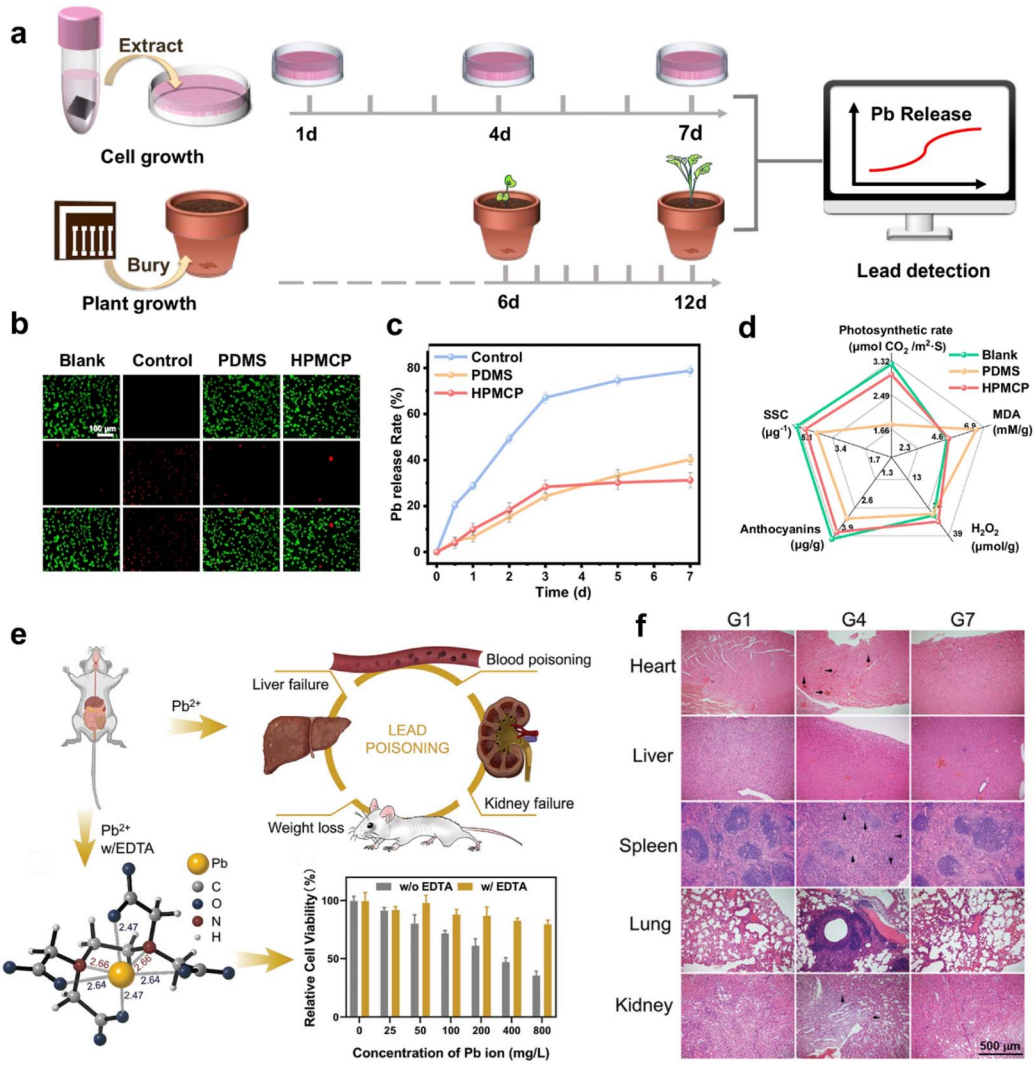

Fig. 8 (a) Schematic illustrations of plant and cell testing methods for evaluating the impact of Pb release from perovskites. (b) The impact of blank, control, PDMS and HPMCP groups on the cell growth performance. Green represents live cells, and red represents dead cells. All scale bars are 100 μm. (c) The lead release rate of the soil at different times with different PSCs buried. (d) Indicators for measuring plant metabolism in blank plants and those grown with PDMS-modified and HPMCP-modified PSCs. Reprinted with permission.[51] Copyright 2025 Springer Nature Limited. (e) Schematic illustration of biotoxicological effects of lead ions in the presence or absence of EDTA Ca–Na, which shows the chelating molecular structure of EDTA with lead ions (with bond lengths in Å), lead poisoning in mice, and the relative cell viability under different concentrations of lead ions with or without EDTA Ca–Na. (f) Hematoxylin and eosin (H&E) staining of the major organs (heart, liver, spleen, lung, and kidney) of Pb-bearing mice in the different treatment groups collected on day 28. Reprinted with permission.[52] Copyright 2024 Wiley-VCH.

for the PDMS group. By analyzing indicators such as photosynthetic rate, malondialdehyde, hydrogen peroxide, anthocyanin, and soluble polysaccharides, it was further found that plants in the PDMS group suffered significant lead damage, whereas the HPMCP group showed nearly identical indicators to the control group, indicating good biocompatibility (Fig. 8d). Wang *et al.* further conducted the first *in vivo* validation of lead toxicity in mice and employed a dual detoxification strategy of "lead sequestration-capture" using calcium disodium ethylenediaminetetraacetate (EDTA Na–Ca). This strategy suppressed lead leakage from perovskites under extreme conditions, and the chelated lead exists in a non-toxic form.[52] Mice were divided into seven groups: control (G1), three lead-exposed untreated groups (G2-G4), and three EDTA-treated groups corresponding to the same lead concentrations (G5-G7). The results showed that untreated mice exhibited toxic symptoms such as sparse hair, reduced water intake, and significant weight loss (Fig. 8e), along with markedly elevated lead levels in blood and major organs. Histopathological examination also revealed apoptosis, necrosis, and inflammatory infiltration (Fig. 8f). In contrast, mice in the EDTA-treated groups showed body weight, organ lead content, and tissue morphology similar to the control group, with no significant abnormalities. This indicates that EDTA Ca–Na can effectively suppress the toxicity of lead from perovskites by chelating lead ions, providing critical *in vivo* toxicological evidence for preventing body weight loss and organ damage, and laying

a foundation for the environmentally friendly commercialization of perovskite photovoltaic devices.

Overall, these studies collectively underscore the shift from conventional physical containment or single-mode adsorption toward integrated strategies that simultaneously address Pb leakage and its inherent toxicity in perovskite photovoltaics. By employing multifunctional materials such as supramolecular cyclodextrins, HPMCP, or chelating agents such as EDTA, researchers have demonstrated effective Pb immobilization coupled with chemical detoxification, transforming Pb^{2+} into stable, low-solubility, and biocompatible forms. These approaches not only suppress Pb release into the environment but also mitigate its biological impact, as validated across multiple models including bacteria, mammalian cells, plants, soil ecosystems, and *in vivo* mice experiments. The integration of "chelation–immobilization–detoxification" mechanisms thus provides a critical pathway to overcome both environmental pollution and bio-toxicity barriers, paving the way for environmentally sustainable perovskite optoelectronic devices.

4 Challenges and limitations of current approaches

Despite significant progress in developing several innovative strategies for Pb sequestration and toxicity mitigation in perovskite optoelectronic, the transition from laboratory validation to industrial applications remains hindered by critical challenges related to scalability, long-term material stability, inherent performance-safety trade-offs and economic feasibility. A comprehensive analysis of these limitations is essential to guide future optimization and ensure sustainable deployment.

4.1 Scalability: bridging laboratory protocols and industrial production

Scalability remains a primary bottleneck for most Pb immobilization strategies. Precise control achievable at the laboratory scale is difficult to replicate in large-area fabrication. For CD-based systems, efficient Pb immobilization depends on well-regulated supramolecular chemistry that generates uniformly distributed Pb-capture sites. While effective on small scales, even minor variations in processing conditions during scale-up can cause nonuniform molecular distribution, resulting in inconsistent defect passivation and Pb sequestration across large-area devices. In addition, CD-modification strategies face additional obstacles in mass production. The precise chemical functionalization needed to enhance Pb capture is difficult to standardize across batches, causing performance variability. Lattice-matching coordination systems face similar scale-up challenges, as the stringent molecular-precision requirements become significantly more difficult and costly to achieve during large-scale synthesis, with impurities and structural heterogeneity severely compromising performance. These challenges are not unique to CD-based or coordination-matching strategies. Across the field, from physical encapsulation to chemical chelation, all the techniques face similar barriers, including inconsistent material performance, difficulties in process standardization, and high costs of maintaining precise control at scale, collectively limiting widespread adoption of these Pb immobilization strategies.

4.2 Long-term stability of Pb-sequestration materials and device longevity

The long-term stability of Pb-sequestration materials under operational stressors including light, heat, and humidity determines their efficacy in preventing Pb leakage throughout the device lifetime. Materials designed to retain Pb^{2+} ions within the perovskite matrix face continuous degradation pressures from environmental and operational factors. Prolonged illumination, thermal cycling, or high humidity may damage their structural integrity or alter chemical reactivity, diminishing their ability to bind Pb^{2+} ions. Th degradation of these materials compromises Pb-immobilization performance, posing risks to environmental safety and device reliability throughout the full-service life. Therefore, understanding the interplay between operational stresses and material stability is essential. The durability of Pb-sequestration mechanisms under realistic conditions ultimately dictates their long-term effectiveness in suppressing Pb release.

4.3 Trade-offs between device performance and environmental impact

Pb-leakage suppression, device performance, and environmental safety are interconnected, often requiring trade-offs. Existing strategies involve implicit compromises. Some chemical-modification networks effectively immobilize Pb but introduce slight barriers to charge transport, reducing key performance metrics of PSCs. Functional groups designed for stronger Pb binding may inadvertently increase defect density, limiting voltage output. Certain lattice-matching coordination systems enhance the stability of specific alloyed perovskites but are incompatible with pure Pb-based perovskites, narrowing their applicability. Other classes of strategies face more pronounced trade-offs. Small-molecule chelators efficiently capture Pb^{2+} but may diffuse to perovskite interfaces, promoting carrier recombination. Pb-replacement strategies such as Sn-based perovskites typically sacrifice efficiency and stability. Biodegradable "green" encapsulation polymers degrade prematurely outdoors, failing to ensure long-term Pb retention. From an environmental perspective, some additives used to enhance hydrophobicity or Pb binding are persistent organic pollutants with bioaccumulation risks. Metal–organic frameworks used in some studies may themselves contain heavy metals, raising secondary pollution concerns when degraded.

4.4 Economic viability: balancing performance and cost

Economic viability is critical for commercial adoption, yet many Pb sequestration strategies substantially increase device cost. CD-based systems require significant material and processing expenses. The synthesis of functionalized CD complexes depends on high-purity reagents and tightly controlled reaction

conditions, markedly increasing the cost of perovskite film fabrication. CD derivatives designed for enhanced Pb-sequestration incur even higher costs due to additional chemical modification steps. Lattice-matched coordination systems demand precise molecular synthesis, further raising costs and limiting large-scale feasibility. Similar cost challenges persist across other approaches. Advanced barrier materials for physical encapsulation require specialized deposition equipment, increasing device-fabrication costs. Small-molecule chelators may require frequent replenishment in large-area modules, raising long-term maintenance costs. Even environmentally beneficial Pb-recycling processes often involve energy-intensive steps that elevate end-of-life treatment costs.

In conclusion, current Pb sequestration strategies face critical challenges in scalability, long-term stability, and economic feasibility, as well as inherent trade-offs between device performance and environmental and biological safety. Addressing these limitations will require interdisciplinary innovations, for instance, improving stability through materials engineering, reducing cost through process optimization, and minimizing environmental impact through green-chemistry design. Only by achieving these breakthroughs can Pb-based perovskite optoelectronics reach their full potential for sustainable deployment.

5 Future research directions

Addressing Pb leakage and toxicity associated with perovskite optoelectronic devices remains a central challenge. Current research has progressed from passive physical isolation to proactive chemical regulation, yet achieving truly sustainable applications still necessitates systematic breakthroughs in material design, alternative compositions, recycling frameworks, and interdisciplinary collaboration. Future development will center around a full-chain objective of "precise capture–safe substitution–circular reuse", advancing multidimensional innovations to resolve Pb toxicity and drive perovskite technologies from laboratory research toward industrial-scale application (Fig. 9). We proposed several future research directions as follows:

5.1 Development of intelligent, stimuli-responsive Pb-chelating materials

The limitations of static chelation mechanisms are increasingly evident, highlighting the need for dynamic regulatory systems adaptable to complex degradation environments. These environments are characterized by fluctuating pH levels, varying temperatures, and diverse coexisting pollutants, all of which can significantly influence chelation efficiency and material stability. Furthermore, the biological toxicity of both Pb ions and the materials themselves must be carefully managed to ensure environmental safety. Intelligent responsive materials are therefore designed to modulate their binding behavior and functionality in reaction to specific environmental stimuli, thereby maintaining high remediation performance while minimizing ecological impact. For instance, CD derivatives incorporating pH-sensitive hydrazone bonds could be developed. Under normal operation, the hydrazone bond remains

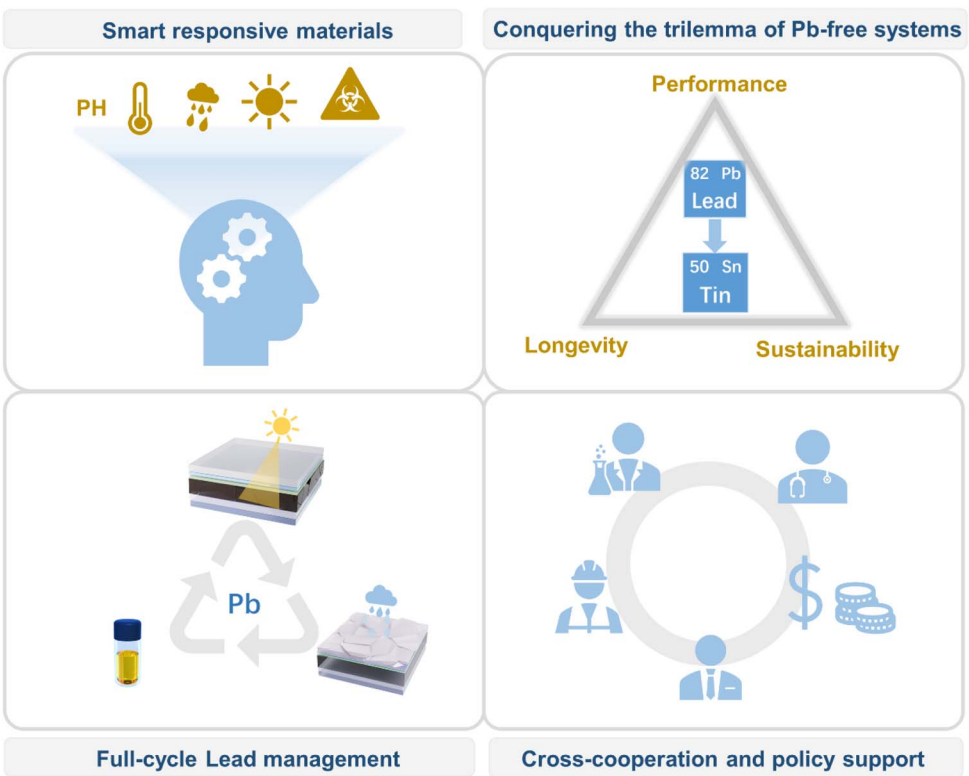

Fig. 9 Future development and directions of this research field.

stable to avoid disturbing the perovskite lattice. Once device damage causes localized acidification (pH < 5), the hydrazone bonds cleaves, releasing additional amino coordination sites to enhance the capture of free Pb^{2+}. Beyond pH-triggered systems, other stimuli-responsive Pb-chelating materials have also shown great promise. Temperature-responsive polymers, for example, can reversibly modulate Pb-binding affinity through phase transition behavior, enabling adaptive performance under fluctuating environmental conditions. Light-responsive chelating networks incorporating azobenzene or spiropyran motifs can achieve on-demand Pb capture and release *via* photoisomerization. In addition, humidity-responsive hydrogels or porous frameworks can dynamically swell to enhance ion diffusion and Pb sequestration during moisture exposure. These diverse responsive mechanisms provide complementary pathways to achieve controllable, energy-efficient, and environmentally adaptive Pb immobilization. Moreover, the construction of hierarchical "nanocage-molecular network" structures will emerge as a key direction to improve Pb capture efficiency. Furthermore, biocompatibility enhancement is also essential. Natural chelators derived from chitosan or gallic acid not only exhibit strong coordination capabilities, but also degrade into metabolites consumable by microorganisms, thus eliminating risks of secondary pollution at the source.

5.2 Research on Pb-free substitution systems

In the research on Pb-free perovskite alternative systems, the key to advancing material iterations lies in systematically addressing the inherent trilemma of performance, longevity, and sustainability. Current studies must not only focus on improving the efficiency and operational lifetime of optoelectronic devices but also fundamentally eliminate the use of Pb, thereby eradicating the long-term risks of Pb leakage. Among the various candidate materials, tin-based perovskites stand out as the most promising candidates due to their desirable optoelectronic properties, which are comparable to those of their Pb-based counterparts. However, their commercialization faces significant challenges. On the one hand, the susceptibility of Sn^{2+} to oxidation leads to material degradation and performance decline, limiting device stability and efficiency. On the other hand, although Pb toxicity is avoided, the potential environmental and biological toxicity introduced by tin itself and other alternative components during synthesis, operation, and disposal still requires comprehensive evaluation. Therefore, achieving truly sustainable Pb-free perovskite technology necessitates adopting an integrated, full-chain strategy covering "material design–fabrication process–device engineering–lifecycle management". This approach must simultaneously suppress Sn^{2+} oxidation and systematically ensure the environmental compatibility of the materials throughout the entire device service cycle, thereby achieving synergistic optimization among performance, stability, and environmental safety. In addition to Sn-based compositions, other lead-free systems such as Bi- and Ge-based perovskite materials have also attracted increasing attention. Bi-based perovskites, including vacancy-ordered $A_3Bi_2X_9$ and double-perovskite $A_2BB'X_6$ structures, exhibit superior moisture and thermal stability owing to their strong Bi–X bonds and rigid frameworks. However, their indirect bandgaps and low carrier mobility still limit their optoelectronic performance. Ge-based perovskites (*e.g.*, $MAGeI_3$ and $CsGeI_3$) possess suitable bandgaps and benign electronic structures but suffer from rapid Ge^{2+} oxidation and instability under ambient conditions. Although both systems remain at the proof-of-concept stage, their low toxicity and structural diversity provide important insights for designing next-generation, environmentally benign halide perovskites.

5.3 Establishing a closed-loop lifecycle management system for Pb-containing species

Constructing a closed-loop life-cycle management framework is essential for sustainable application of perovskite optoelectronics. This requires interventions across multiple stages. During the device design stage, it is desirable to introduce degradable "sacrificial layers" such as a polyvinyl alcohol–hydroxyapatite interlayer between the perovskite and electrodes. After device end-of-life, immersing the module in a mildly acidic solution dissolves this layer and release Pb^{2+} ions, thereby enhancing the recyclability of ITO glass and metal electrodes. Innovations in recycling processes can focus on multi-component separation strategies. For instance, "selective dissolution" technology employs organic acids (*e.g.*, citric acid) to preferentially dissolve the Pb-based inorganic phase within the perovskite lattice without damaging the electrodes or substrates. By adjusting the solution pH, Pb^{2+} ions can be separated as insoluble PbC_2O_4 precipitates, thus improving the recovery rates of Pb components. Another attempt, an "electrochemical deposition recycling" method can be considered, whereby crushed devices are immersed in an electrolyte solution, and a constant voltage is then applied to direct the deposition of Pb^{2+} ions onto the cathode, forming high-purity Pb foil. These pieces of foil can be reused in perovskite precursor preparation, reducing dependence on primary Pb resources. Furthermore, real-time monitoring systems integrated with fluorescent probes will be helpful. When encapsulation damage causes Pb leakage above 15 ppb, rhodamine-functionalized nanosensors immediately emit fluorescent warnings, enabling precise environmental risk management. Through innovations in material design, separation technologies, and monitoring systems, these strategies establish a "design–recycling–monitoring" full-chain management framework, enabling true closed-loop recycling for Pb-based perovskite optoelectronic devices. It should be noted that most of the aforementioned recycling and recovery approaches are still at the proof-of-concept or pilot scale. Therefore, future efforts should incorporate lifecycle assessment-informed criteria, including recovery purity and yield, energy and chemical footprints, compatibility with manufacturing lines, and potential secondary pollution risks, to enable a realistic and quantitative evaluation of their feasibility, scalability and sustainability.

5.4 Interdisciplinary collaboration, equipment upgrades, standard setting, and policy support

Interdisciplinary cooperation and standardized frameworks are foundational for successful technological deployment. Materials scientists need to collaborate with toxicologists to develop models correlating chemical speciation with biological toxicity, which not only evaluate Pb^{2+} ion concentrations but also quantify the ecological impact of chelated Pb^{2+} on algae and soil microorganisms, thereby avoiding cases where materials meet regulatory limits yet remain biologically harmful. On the industrial side, full-process cost optimization is essential, such as roll-to-roll fabrication of Pb-chelating perovskite films to lower per-square-meter manufacturing costs. Modular encapsulation technologies compatible with existing photovoltaic production lines should be developed to minimize equipment-retrofit expenses and keep Pb-safety costs within a viable range, thereby balancing environmental performance and mass-production feasibility. At the policy level, establishing a Pb-safety certification system for perovskite optoelectronic devices is urgently needed. Tax incentives should be granted to enterprises adopting closed-loop Pb-recycling technologies, creating a positive cycle from technological innovation to market incentives."

In conclusion, future research can achieve precise Pb capture through intelligent materials design, breakthrough the performance bottlenecks of Pb-free systems by virtue of chemical engineering, and establish resource circulation and reuse *via* a closed-loop recycling pathway. Ultimately, with the support of interdisciplinary collaboration and policies, perovskite technology will truly become a next-generation optoelectronic benchmark that integrates high performance and environmental friendliness, reflecting its comprehensive value in both technological advancement and ecological sustainability.

Author contributions

W.-Q. W. conceived the concept and provided overall guidance. G. L. performed the main literature analysis, drafted the manuscript, and prepared most of the figures. G. Y. and W. F. contributed to selected sections and/or figures and participated in manuscript revision. All authors discussed the content and approved the final version.

Conflicts of interest

The authors declare that they have no conflicts of interest.

Data availability

No primary research results, software, or code have been included, and no new data were generated or analyzed as part of this perspective.

Acknowledgements

The authors acknowledge the financial support from the National Key R&D Program of China (2025YFE0106500), the Guangzhou Science and Technology Programme (2024B03J1227), the Guangdong Basic and Applied Basic Research Foundation (2023B1515120008 and 2024A1515011571) and the National Natural Science Foundation of China (52472115).

References

1 Y. Lin, Z. Lin, S. Lv, Y. Shui, W. Zhu, Z. Zhang, W. Yang, J. Zhao, H. Gu, J. Xia, D. Wang, F. Du, A. Zhu, J. Liu, H. Cai, B. Wang, N. Zhang, H. Wang, X. Liu, T. Liu, C. Kong, D. Zhou, S. Chen, Z. Yang, T. Li, W. Ma, G. Fang, L. Echegoyen, G. Xing, T. Yang, W. Cai, M. Li, W. Huang and C. Liang, *Nature*, 2025, **642**, 78.
2 National Renewable Energy Laboratory. Best Research-Cell Efficiency Chart. https://www.nrel.gov/pv/cell-efficiency.html.
3 T. Kirchartz, *Chem. Sci.*, 2025, **16**, 8153.
4 X. Ji, Y. Zhao, X. Chen, S. Zhang, L. Zhan, H. Zhang, W. Zheng, W.-H. Zhu and Y. Wu, *Chem. Sci.*, 2025, **16**, 8569.
5 W. Feng, X. Liu, G. Liu, G. Yang, Y. Fang, J. Shen, B. Jin, X. Chen, Y. H. Huang, X. D. Wang, C. Wu, S. Yang and W.-Q. Wu, *Angew. Chem., Int. Ed.*, 2024, **136**, e202403196.
6 G. Yang, J. Sun, X. Chang, C. Yu, G. Liu, Y. Fang, H. Chen, Y. H. Huang, H. Liu, J. Fang, L. Wang, Y. Tan, W. Feng, M. Yang, Y. Feng, J.-X. Zhong, D. Gulamova, Y. Fang, C. Wu, L. Qiu, X.-D. Wang, Z. Yang and W.-Q. Wu, *Adv. Mater.*, 2025, e12129.
7 J. Liang, X. Hu, C. Wang, C. Liang, C. Chen, M. Xiao, J. Li, C. Tao, G. Xing, R. Yu, W. Ke and G. Fang, *Joule*, 2022, **6**, 816.
8 Y. Gao, F. Ren, D. Sun, S. Li, G. Zheng, J. Wang, H. Raza, R. Chen, H. Wang, S. Liu, P. Yu, X. Meng, J. He, J. Zhou, X. Hu, Z. Zhang, L. Qiu, W. Chen and Z. Liu, *Energy Environ. Sci.*, 2023, **16**, 2295.
9 D. R. Ortega, D. F. G. Esquivel, T. B. Ayala, B. Pineda, S. G. Manzo, J. M. Quino, P. C. Mora and V. P. de la Cruz, *Toxics*, 2021, **9**, 23.
10 X. Zeng, Z. Zeng, Q. Wang, W. Liang, Y. Guo and X. Huo, *J. Hazard. Mater.*, 2022, **434**, 128842.
11 C. H. Chen, S. N. Cheng, L. Cheng, Z. K. Wang and L. S. Liao, *Adv. Energy Mater.*, 2023, **13**, 2204144.
12 Y. Jiang, L. Qiu, E. J. Juarez-Perez, L. K. Ono, Z. Hu, Z. Liu, Z. Wu, L. Meng, Q. Wang and Y. Qi, *Nat. Energy*, 2019, **4**, 585.
13 S. Chen, Y. Deng, X. Xiao, S. Xu, P. N. Rudd and J. Huang, *Nat. Sustain.*, 2021, **4**, 636.
14 X. Jin, Y. Yang, T. Zhao, X. Wu, B. Liu, M. Han, W. Chen, T. Chen, J.-S. Hu and Y. Jiang, *ACS Energy Lett.*, 2022, **7**, 3618.
15 Q. Wang, Z. Lin, Y. Xu, B. Zhang, X. Guo, Z. Hu, Y. Hao and J. Chang, *EcoMat*, 2023, **5**, e12400.
16 G. Liu, G. Yang, W. Feng, H. Li, M. Yang, Y. Zhong, X. Jiang and W.-Q. Wu, *Adv. Mater.*, 2024, **36**, 2405860.
17 K. Liu, T. Hu, Z. Cai, F. Liu, S. Rafique, X. Li, L. Deng, C. Li, Y. Wang, Q. Guo, X. Yue, J. Wang, Y. Yang, C. Cong, s. Chen, J. Zhang, A. Yu and Y. Zhan, *Energy Environ. Sci.*, 2024, **17**, 5576.
18 H. Liu, Z. Zhang, Y. Shi, W. Ran, H. Zhong and F. Zhang, *Joule*, 2025, **9**, 101816.

19 H. Luo, J. Ma, P. Gao, S. Wang, R. Zhao, J. Yang, Y. Li, P. Zhou, Q. Xu, R. Zhu, Z. Liu, X. Li, W. Chen, Y. Song and Y. Zhang, *Adv. Mater.*, 2025, 2506206.
20 Y. Xu, Q. Wang, Z. Lin, S. Zhang, X. Guo, Z. Hu, J. Xiao, Y. Hao, L. Ding and J. Chang, *Interdiscipl. Mater.*, 2025, **4**, 599.
21 G. Zhang, Y. Zheng, H. Wang, G. Ding, F. Yang, Y. Xu, J. Yu and Y. Shao, *Joule*, 2024, **8**, 496.
22 X. Xiao, M. Wang, S. Chen, Y. Zhang, H. Gu, Y. Deng, G. Yang, C. Fei, B. Chen, Y. Lin, M. D. Dickey and J. Huang, *Sci. Adv.*, 2021, **7**, eabi8249.
23 T. Wang, Z. Wan, X. Min, R. Chen, Y. Li, J. Yang, X. Pu, H. Chen, X. He, Q. Cao, G. Feng, X. Chen, Z. Ma, L. Jiang, Z. Liu, Z. Li, W. Chen and X. Li, *Adv. Energy Mater.*, 2024, **14**, 2302552.
24 X. Tang, T. Zhang, W. Chen, H. Chen, Z. Zhang, X. Chen, H. Gu, S. Kang, C. Han, T. Xu, J. Cao, J. Zheng, X. Ou, Y. Li and Y. Li, *Adv. Mater.*, 2024, **36**, 2400218.
25 J. Suo, H. Pettersson and B. Yang, *EcoMat*, 2025, **7**, e12511.
26 Q. Zhuang, Z. Xu, H. Li, C. Zhang, C. Gong, H. Wang, X. Li and Z. Zang, *Sci. Adv.*, 2025, **11**, eado7318.
27 J. Dou, Y. Bai and Q. Chen, *Mater. Chem. Front.*, 2022, **6**, 2779.
28 X. Meng, X. Hu, Y. Zhang, Z. Huang, Z. Xing, C. Gong, L. Rao, H. Wang, F. Wang, T. Hu, L. Tan, Y. Song and Y. Chen, *Adv. Funct. Mater.*, 2021, **31**, 2106460.
29 R. Tan, Z. Liu, Z. Zang and S. Zhao, *Chem. Sci.*, 2025, **16**, 2136.
30 G. Liu, X. Jiang, Y. He, C. H. Kuan, G. Yang, W. Feng, X. Chen and W.-Q. Wu, *Angew. Chem., Int. Ed.*, 2025, **137**, e202419183.
31 G. Liu, X. Jiang, W. Feng, G. Yang, X. Chen, Z. Ning and W.-Q. Wu, *Angew. Chem., Int. Ed.*, 2023, **62**, e202305551.
32 G. Liu, Y. Zhong, W. Feng, M. Yang, G. Yang, J. X. Zhong, T. Tian, J. B. Luo, J. Tao, S. Yang, X.-D. Wang, L. Tan, Y. Chen and W.-Q. Wu, *Angew. Chem., Int. Ed.*, 2022, **61**, e202209464.
33 H. Zhou, W. Sheng, H. Rao, Y. Su, W. Zhu, Y. Zhong, Y. Liu, J. He, L. Tan and Y. Chen, *Angew. Chem., Int. Ed.*, 2025, **137**, e202422217.
34 H. Zhou, H. Rao, Y. Jin, W. Zhu, Z. Deng, Y. Zhong, W. Sheng, G. Liu, L. Tan and Y. Chen, *Angew. Chem., Int. Ed.*, 2025, e202513416.
35 M. Ma, X. Jiang, Z. Zang, X. Wen, W. Zhou, H. Wu, S. Peng, Y. Liu, H. Li, D. Yu, H. Liang, H. Wang, W. Zhou, Z. Su, F. Zheng, X. Guo, A. V. Emeline, C. C. Stoumpos and Z. Ning, *Adv. Funct. Mater.*, 2024, **34**, 2407095.
36 Z. Zhu, X. Jiang, D. Yu, N. Yu, Z. Ning and Q. Mi, *ACS Energy Lett.*, 2022, **7**, 2079.
37 W. Ning and F. Gao, *Adv. Mater.*, 2019, **31**, 1900326.
38 T.-S. Su, A. Krishna, C. Zhao, J. Chu and H. Zhang, *Chem. Soc. Rev.*, 2025, **54**, 6448.
39 C. Zhao, Z. Zhou, M. Almalki, M. A. Hope, J. Zhao, T. Gallet, A. Krishna, A. Mishra, F. T. Eickemeyer, J. Xu, Y. Yang, S. M. Zakeeruddin, A. Redinger, T. J. Savenije, L. Emsley, J. Yao, H. Zhang and M. Graetzel, *Nat. Commun.*, 2024, **15**, 7139.
40 H. Song, H.-B. Kim, S. C. Cho, J. Lee, J. Yang, W. H. Jeong, J. Y. Won, H. I. Jeong, J. Yeop, J. Y. Kim, B. J. Lawrie, M. Ahmadi, B. R. Lee, M. Kim, S. J. Choi, D. S. Kim, M. Lee, S. U. Lee, Y. Jo and H. Choi, *Joule*, 2024, **8**, 2283.
41 S. Masi, F. Aiello, A. Listorti, F. Balzano, D. Altamura, C. Giannini, R. Caliandro, G. Uccello-Barretta, A. Rizzo and S. Colella, *Chem. Sci.*, 2018, **9**, 3200.
42 S. V. Dummert, H. Saini, M. Z. Hussain, K. Yadava, K. Jayaramulu, A. Casini and R. A. Fischer, *Chem. Soc. Rev.*, 2022, **51**, 5175.
43 M. Yang, T. Tian, Y. Fang, W.-G. Li, G. Liu, W. Feng, M. Xu and W.-Q. Wu, *Nat. Sustain.*, 2023, **6**, 1455.
44 Ministry of Ecology and Environment of the People's Republic of China. *Standards for drinking water quality*. **GB** 5749–2006.
45 USA Environmental Protection Agency, https://www.epa.gov/ground-water-and-drinking-water/national-primary-drinking-water-regulations#one, accessed: May 2009.
46 T. Tian, M. Yang, Y. Fang, S. Zhang, Y. Chen, L. Wang and W.-Q. Wu, *Nat. Commun.*, 2023, **14**, 234.
47 D. Li, C. Du, B. Hu, Z. Xing, X. Hu, T. Hu and Y. Chen, *Adv. Funct. Mater.*, 2025, **36**, e13938.
48 M. Yang, Y. Tan, G. Yang, X. Chang, T. Tian, W. G. Li, Y. Fang, J. Shen, S. Yang and W.-Q. Wu, *Angew. Chem., Int. Ed.*, 2025, **137**, e202415966.
49 J. Wang, X.-Y. Dai, L. Bi, J. Sun, M. Liu, X. Ji, F. R. Lin, Q. Fu and A. K.-Y. Jen, *Joule*, 2025, **9**, 102105.
50 J.-X. Zhong, M.-C. Chen, Y. Tan, Y.-T. Xiao, G. Yang, H. Chen, S.-W. Fan, J.- Yi Yang, W. Zou, J. Tao, Dr Y. Zhou, R. Liu, W.-Q. Xu, X. Chang, D.-B. Kuang and Wu-Q. Wu, *Angew. Chem., Int. Ed.*, 2025, **64**, e202518552.
51 Y. Yang, J. Zhao, H. Yang, X. Yang, Y. Lu, Z. Huang, S. Duo, Z. Xiong and X. Hu, *Nat. Commun.*, 2025, **16**, 8993.
52 C.-H. Chen, S.-N. Cheng, F. Hu, Z.-H. Su, K.- Li Wang, L. Cheng, J. Chen, Y.-R. Shi, Y. Xia, T.-Y. Teng, X.-Y. Gao, I. Yavuz, Y.-H. Lou and Z.-K. Wang, *Adv. Mater.*, 2024, **36**, 2403038.